Journal of Crohn's and Colitis, 2019, 1–17
doi:10.1093/ecco-jcc/jjz170
Advance Access publication October 20, 2019
Original Article

Original Article

The TLR9 Agonist Cobitolimod Induces IL10-Producing Wound Healing Macrophages and Regulatory T Cells in Ulcerative Colitis

Heike Schmitt,[a] Julia Ulmschneider,[a] Ulrike Billmeier,[a] Michael Vieth,[b] Patrizio Scarozza,[a,c] Sophia Sonnewald,[d] Stephen Reid,[d] Imke Atreya,[a] Timo Rath,[a] Sebastian Zundler,[a] Melanie Langheinrich,[e] Jürgen Schüttler,[f] Arndt Hartmann,[g] Thomas Winkler,[d] Charlotte Admyre,[h] Thomas Knittel,[h] Christine Dieterich Johansson,[h] Arezou Zargari,[h] Markus F. Neurath,[a*] Raja Atreya[a*]

[a]First Department of Medicine, Friedrich-Alexander-University Erlangen-Nürnberg, Erlangen, Germany [b]Institute of Pathology, Klinikum Bayreuth, Bayreuth, Germany [c]Internal Medicine Department, University Tor Vergata, Rome, Italy [d]Department of Biology, Friedrich-Alexander-University Erlangen-Nürnberg, Erlangen, Germany [e]Department of Surgery, Friedrich-Alexander-University Erlangen-Nürnberg, Erlangen, Germany [f]Department for Anesthesiology, Friedrich-Alexander-University Erlangen-Nürnberg, Erlangen, Germany [g]Department of Pathology, Friedrich-Alexander-University Erlangen-Nürnberg, Erlangen, Germany [h]InDex Pharmaceuticals, Tomtebodavägen 23a, SE-171 77 Stockholm, Sweden

*These authors contributed equally.

Corresponding author: Prof. Raja Atreya, MD, First Department of Medicine, Friedrich-Alexander-University Erlangen-Nürnberg, Ulmenweg 18, 91054 Erlangen, Germany. Tel: 49 9131 85 35115; Fax: 49 9131 85 35116; Email: raja.atreya@uk-erlangen.de.

Conference: Part of this work was presented at Digestive Disease Week [DDW] in Washington [2018] and Congress of European Crohn's and Colitis Organisation [ECCO] in Vienna [2018] and FALK Symposium 214 in Oxford [2019].

Abstract

Background and Aims: The topically applied Toll-like receptor 9 [TLR9] agonist cobitolimod is a first-in-class DNA-based oligonucleotide with demonstrated therapeutic efficacy in clinical trials with ulcerative colitis [UC] patients. We here characterized its anti-inflammatory mechanism in UC.
Methods: Luminal cobitolimod administration was evaluated in an experimental dextran sodium sulfate [DSS]-induced colitis model. Cultured blood and mucosal cells from UC patients were treated with cobitolimod and analysed via microarray, quantitative real-time PCR, ELISA and flow cytometry. Intestinal slides of cobitolimod-treated UC patients were analysed by immunohistochemistry.
Results: Cobitolimod administration markedly suppressed experimental colitis activity, and microarray analyses demonstrated mucosal IL10 upregulation and suppression of IL17 signalling pathways. Cobitolimod treatment was associated with significant induction of mucosal IL10+Tr1 and Treg cells and suppression of Th17 cells. TLR9 knockout mice indicated that cobitolimod requires TLR9 signalling for IL10 induction. In UC patients, mucosal TLR9 levels correlated with severity of inflammation. Cobitolimod inhibited IL17A and IL17F, but increased IL10 and FoxP3 expression in cultured intestinal UCT cells. Cobitolimod-mediated suppression of intestinal IL17+T cells was abrogated by IL10 blockade. Furthermore, cobitolimod led to heightened IL10 production

by wound healing macrophages. Immunohistochemistry in intestinal biopsies of cobitolimod-treated UC patients indicated increased presence of IL10+mononuclear and regulatory T cells, as well as reduction of IL17+cells.

Conclusion: Activation of TLR9 via cobitolimod might represent a novel therapeutic approach in UC, as it suppresses Th17 cells and induces anti-inflammatory IL10+macrophages and regulatory T cells, thereby modifying the dysregulated intestinal cytokine balance.

Podcast: This article has an associated podcast which can be accessed at https://academic.oup.com/ecco-jcc/pages/podcast
Key Words: Ulcerative colitis; TLR9; cobitolimod

1. Introduction

Inflammatory bowel disease [IBD] encompasses chronic inflammatory disorders of the gastrointestinal tract whose phenotypic spectrum mainly comprises Crohn's disease [CD] and ulcerative colitis [UC]. UC is characterized by a superficial, continuous mucosal and submucosal inflammation, which is mainly limited to the large intestine.[1,2] The development of targeted therapies, such as anti-tumour necrosis factor [anti-TNF] antibodies [infliximab, adalimumab, golimumab], anti-adhesion molecule antibodies [vedolizumab] and recently JAK-inhibitors [tofacitinib], has significantly improved therapeutic options in UC. Nevertheless, a large proportion of patients remain primarily unresponsive or show loss of response to these therapies.[3] There is therefore urgent clinical need for the development of novel therapies with an alternative mode of action.

A perturbed homeostasis between commensal bacteria and mucosal immunity has been identified as a critical determinant in UC pathogenesis. Specifically, aberrant modulation of Toll-like receptors [TLRs] has been implicated in driving mucosal inflammation.[4] It has been shown that TLRs not only control innate immunity but also critically regulate subsequent adaptive immunity, such as T cell activation, indicating that TLR signalling plays a pleiotropic role in the induction of intestinal inflammation.[5,6]

The intracellular receptor TLR9 recognizes the unmethylated dinucleotide CpG, which has been identified as the main immunostimulatory component in bacterial and viral DNA. TLR9 is expressed in antigen-presenting cells such as macrophages, dendritic cells and B cells but also on intestinal epithelial cells, where it is expressed on both the apical and the basolateral sides of the cell.[7] Whereas apical stimulation of TLR9 results in tolerance, activation on the basolateral side stimulates NFκB and induces the secretion of IL8.[8] Interestingly, TLR9-deficient mice developed more severe colitis following challenge with dextran sodium sulfate [DSS], compared to wild-type controls.[9,10] Severity of colitis was significantly attenuated after the transfer of T cells into immunosuppressed RAG-mice, when donor mice were treated with a TLR9 agonist prior to the transfer, indicating that a regulatory T cell pool was induced via TLR9 signalling.[11] Correspondingly, CpG-site-containing oligodeoxynucleotides [ODNs] suppressed immune cell activation and protected barrier function in experimental colitis via TLR9 signalling.[12] Additionally, an increased production of the anti-inflammatory cytokine IL10 by regulatory dendritic cells and macrophages was observed after stimulation with TLR9 agonists *in vitro*, which is in line with the constitutive interaction of CD14+macrophages with the MyD88-dependent TLR7 and TLR9 pathways.[13]

Consistent with these data obtained in experimental colitis models, a pivotal role of TLR9 signalling could similarly be demonstrated in UC patients, as there was a positive correlation between the severity of endoscopic and histological inflammation and mucosal TLR9 mRNA expression.[14] In inflammatory circumstances, TLR9 agonists act by both decreasing the enormous immune activation, especially in IBD, and setting the balance of the Th1/Th2 immune response. Due to complex signalling of ODN binding TLRs [including TLR9] a dynamic regulation of pro- and anti-inflammatory cytokines is present. Although the ability of TLR activation to exert a protective effect against intestinal inflammation has been noted, there are also contrasting data that indicate a CpG-dependent perpetuation of chronic mucosal inflammation.[10,15]

The role of regulatory T cells [Tregs] in the maintenance of intestinal homeostasis is supported by the demonstration that a lack of Tregs is associated with development of intestinal inflammation. Several studies have demonstrated that Tregs were reduced in blood and colonic mucosa of UC patients while IL17/Th17 levels were significantly upregulated compared to healthy controls. Together, the dysregulation of the Th17/Treg balance has been shown to play a crucial role in the development and perpetuation of UC.[16–19]

The single stranded DNA-based immunomodulatory sequence [DIMS] cobitolimod, which contains an unmethylated CpG motif, has been shown to activate the TLR9 on target cells such as lymphocytes or antigen presenting cells [APCs] *in vitro* with potent induction of anti-inflammatory cytokines, such as IL10 and type I interferons.[20]

Cobitolimod showed therapeutic efficacy upon topical application in refractory UC patients in a proof of concept study and in a recently published clinical trial.[21,22] Cobitolimod application was well tolerated. These results prompted an ongoing phase IIb trial, in which cobitolimod is repeatedly administered over 3 weeks [NCT03178669].

Based on the above described findings, we investigated the molecular mechanism of action of the TLR9 agonist cobitolimod in intestinal inflammation, as it might represent a unique novel therapeutic approach in UC patients.

2. Material and methods

2.1 Patients

In total, 112 UC patients were analysed across all experiments. In some patients, intestinal tissue as well as blood samples were taken for analysis. Intestinal biopsies or gut specimens from UC patients [n = 83; 45 female, 23–71 years and 38 male, 19–74 years] were used for cell culture [n = 70] or RNA isolation [n = 13] studies. Peripheral blood mononuclear cells [PBMCs] were isolated from blood of 47 UC patients [24 female, 24–56 years; 23 male, 22–59 years] and from buffy coats of nine healthy donors.

In addition to above described non-cobitolimod-treated UC patients, histological slides of colon biopsies were obtained from UC patients who had participated in the placebo-controlled, double-blind, randomized multi-centre clinical study CSUC-01/10 [NCT01493960],

where the efficacy and safety of cobitolimod was assessed. In this clinical trial, 131 UC patients with treatment-refractory UC were included with active clinical [Clinical Activity Index score ≥ 9] and endoscopic [Mayo endoscopic subscore > 1] disease. Cobitolimod [30 mg] was administered on weeks 0 and 4 proximal to the site of the most severe inflamation or, in the case of pancolitis, in the transverse colon via topical endoscopic application. Biopsies were taken from the area of most severe endoscopic inflammation at week 0 and in the same area again at week 4. Histological slides of colon biopsies from baseline [week 0] and week 4 were obtained from placebo- [n = 4] and cobitolimod-treated patients responding [n = 7] or not responding [n = 6] to cobitolimod treatment [see Figure 8]. The placebo patients had an unchanged endoscopic Mayo subscore [≥ 2] at weeks 0 and 4, and did therefore not respond endoscopically to placebo treatment. The cobitolimod patients were endoscopic responders to cobitolimod application at baseline, as they demonstrated endoscopic response [endoscopic Mayo subscore of 0 or 1] in the follow-up endoscopy at week 4. Samples were included in the study after obtaining prior written informed consent from each patient, and sample collection was previously approved by the ethical committee and the institutional review board of the University of Erlangen-Nürnberg.

2.2 Disease classification of UC patients

A pathologist blinded to all clinical and endoscopic data of the respective patient performed histological classification of the intestinal biopsies from UC patients [Figure 1A]. Severity of inflammation was determined by histopathological grading that included absent [score 0], mild [score 1], moderate [score 2] and severe [score 3] inflammation. The currently available validated histopathological scores for UC [Nancy-Index and Robarts Histopathology Index] were not used for evaluation by the pathologist. The endoscopic Mayo score was used for the assessment of the severity of endoscopic inflammation in the examined UC patients.[23] The partial Mayo score was used for the assessment of the clinical disease activity of the UC patients at the time of endoscopic examination.[24] The clinical, endoscopic and histological activity scores of the UC patients from Figure 1A are depicted in Supplementary Table 1.

2.3 Mice

Balb/c mice were obtained from Charles River Laboratories, Research Models and Services. TLR9 knockout mice were originally obtained from Hermann Wagner and kindly provided by Thomas Winkler. Eight-week-old female Balb/c mice were used for the experiments and were kept in individually ventilated cages in compliance with the Animal Welfare Act. Water and food were available *ad libitum*. Mice were randomly mixed per cage before initiation of the experiment to ensure comparable experimental conditions. Animal experiments were performed in accordance with German laws for the protection of animals, after approval by the animal welfare committee [Regierung von Unterfranken].

2.4 DSS-induced colitis

For DSS-induced colitis, 3% [w/v] DSS [MP Biomedicals] was added to the drinking water of 8-week-old female Balb/c mice for 10 days. An additional control group of three mice which were not given DSS [untreated] was also part of the experimental set up.

2.5 Rectal administration of cobitolimod or placebo

Groups of seven mice were rectally administered with 40, 84 or 250 µg cobitolimod on days 4 and 8. The respective concentration of cobitolimod was diluted with sterile water and 100 µL was used for rectal administration per mouse. Mice in the placebo group [n = 7] were treated with 100 µL sterile water only. The three mice from the untreated group [no DSS] were not given cobitolimod or water rectally.

2.6 Evaluation of DSS-induced colitis

Food uptake and body weight were monitored on days 0, 2, 4, 6, 7, 8 and 10. The Disease Activity Index [DAI] is the combined score of body weight loss compared to initial body weight, stool consistency and visible blood in faeces. The maximum score per mouse is 12.[25,26] DAI was assessed on days 0, 2, 4, 6, 7, 8 and 10. In addition, colonic inflammation was studied *in vivo* using the Coloview endoscopic system consisting of a miniature endoscope [scope 1.9 mm outer diameter], a xenon light source, a triple chip camera and an air pump [all from Karl Storz] to achieve regulated inflation of the mouse colon. For endoscopy, mice were anaesthetized with 4% isoflurane in 100% oxygen at a rate of 0.2–0.5 L/min [2% isoflurane was used for maintenance]. The modified murine endoscopic score of colitis severity [MEICS] were used to determine endoscopic signs of inflammation.[27] The endoscopic colitis grading [MEICS score] consists of the following five parameters: thickening of the colon, change of the normal vascular pattern, presence of fibrin, mucosal granularity and stool consistency. Endoscopic grading was performed for each parameter [score 0–3] leading to an accumulative score between 0 and 15.[27] Endoscopic grading was analysed on days 0, 2, 4, 6, 7, 8 and 10. Histological severity of inflammation was assessed by histopathological analysis of intestinal sections. The histological score encompassed 0 = no inflammation, 1 = remission, 2 = mild inflammation, 3 = moderate inflammation and 4 = severe inflammation.[28]

2.7 Isolation of RNA and qRT-PCR

For quantitative real-time PCR [qRT-PCR] RNA was isolated from intestinal biopsies of mice treated with DSS or from UC patients using the Nucleo Spin II kit [Macherey-Nagel]. In total, 1 µg RNA was reverse transcribed into cDNA [iScript, BioRad] according to the manufacturer's instructions. For quantitative expression analysis, quantitect primers [Qiagen] were used. Data were normalized to the housekeeping-gene HPRT.

2.8 Microarray experiments

Intestinal biopsies were taken from DSS-induced colitis mice that were treated with placebo [n = 4] or cobitolimod [n = 4] as mentioned above. Lamina propria mononuclear cells [LPMCs] were isolated and RNA was extracted. Its integrity was verified using a Nano Chip [RNA 6000; Agilent Technologies] on a BioAnalyzer [vB.02.03 BSI307; 2100; Agilent Technologies] as recommended by the manufacturer's protocol [RNA 6000 Nano Assay Protocol2]. Sample labelling and preparation for microarray hybridization was performed according to a standard protocol. The RNA replicates of four placebo and four cobitolimod-treated mice in DSS colitis were each hybridized onto a 4 × 44k array [design-ID 026655; Agilent Technologies]. Data were extracted with the feature extraction software package [v.11.7.1; Agilent Technologies] using a standard protocol.[29] The text files generated by the feature extraction software were imported into GeneSpring GX [v.12.5; Silicon Genetics]. Data were $\log_2$-transformed followed by normalization to the 75th percentile and corrected to the median of all samples. Features passing the quality check [flags detected in at least one condition] and showing changes in expression levels equal to or greater than two-fold were

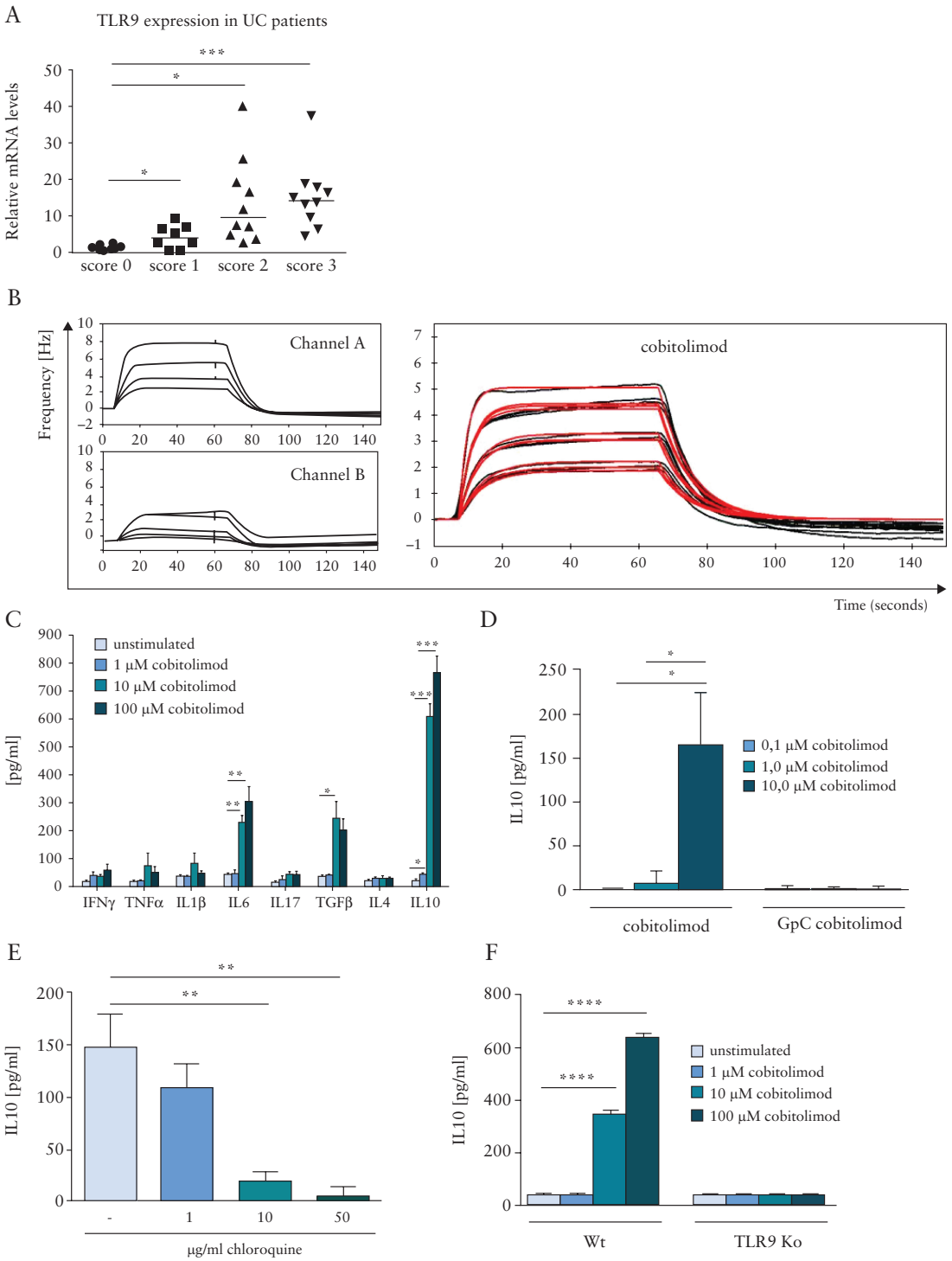

Figure 1. TLR9 expression levels in ulcerative colitis [UC] patients and activation of the TLR9 pathway by cobitolimod. [A] qRT-PCR was performed on intestinal biopsies from UC patients with absent [score 0, n = 8], mild [score 1, n = 8], moderate [score 2, n = 10] or severe [score 3, n = 10] inflammation. Severity of inflammation was determined by histopathological grading. Data were normalized to the housekeeping-gene HPRT and compared to the control group without mucosal inflammation [score 0]. Every symbol represents a single patient. Median value is indicated as a line. [B] Sensograms of *in vitro* binding of cobitolimod to the human TLR9. A polystyrene surface [PS] with TLR9 and liposomes were docked in channel A [upper left], whereas a PS surface with a control mock protein and liposomes were docked in channel B [lower left]. Cobitolimod was injected in duplicate at different concentrations [200, 100, 50, 25 µg/mL] into both channels. The sensograms obtained from channel A were subtracted from the signal obtained from the reference surface in channel B. [C] LPMCs isolated from colon of UC patients [n = 8] were untreated or treated for 48 h with different concentrations of cobitolimod. Release of different cytokines in the supernatant was determined by ELISA. [D] PBMCs isolated from healthy donors [n = 4] were stimulated for 48 h with different concentrations of cobitolimod or GpC cobitolimod [cobitolimod with GpC instead of a CpG motif]. Release of IL10 was determined by cytometric bead array [CBA]. [E] PBMCs isolated from healthy donors [n = 5] were pre-incubated for 45 min either with medium alone or with 1, 10 or 50 µg/mL chloroquine. After pre-incubation, 100 µM cobitolimod was added to each well. Release of IL10 was determined using the CBA method. [F] Isolated splenocytes from wildtype [wt, n = 6] or TLR9 knock-out mice [TLR9 ko, n = 6] were untreated or treated for 48 h with different concentrations of cobitolimod. Release of IL10 was determined by ELISA. Data in C–F represent mean values ± SD. *$p \leq 0.05$; **$p \leq 0.01$; ***$p \leq 0.001$; ****$p \leq 0.0001$.

selected for further analysis. A volcano plot was applied to identify statistically significant [$p > 0.05$], more than two-fold differentially expressed genes, between two conditions, including the Benjamini–Hochberg multiple test correction. Pearson and Ward analyses were used to generate hierarchical clustering of the experimental conditions [placebo or cobitolimod-treated mice in DSS-induced colitis]. The heatmap depicts genes that have been described in the literature to be susceptible regarding DSS-induced colitis.[30–32]

2.9 Immunofluorescence

Cryo-frozen intestinal cross sections from patient colonic biopsies were fixed with 4% paraformaldehyde and stained using the TSA plus kit [Perkin Elmer] according to the manufacturer's instructions. Alternatively, slides were fixed with methanol at –20°C for 10 min, blocked with 10% fetal calf serum [FCS]/1% bvine serum albumin for 1 h and incubated overnight at 4°C with the primary antibody. Paraffin-embedded tissues were deparaffinized and antigen unmasking was performed using citrate buffer. Thereafter slides were incubated with different antibodies.

For DSS-induced colitis mice, immunofluorescence analysis was performed in intestinal sections, which were taken at the end of the experiment on day 10 for IL10 [Abcam], IL17 [Abcam] and Foxp3 [eBioscience]. Colon biopsies of UC patients were taken before and 28 days after topical cobitolimod or placebo treatment[21,22] and the corresponding cross sections were stained for IL10 [Abcam], FoxP3 [eBioscience] or IL17 [Abcam]. From each sample, four to six high power fields [HPFs] per patient were analysed using a 10× objective magnification. Analysis of images was done with a fluorescence microscope [BZ-8100 or BZ-9000, Keyence] or a confocal microscope [LSM, Leica Microsystems] and calculated with ImageJ 1.52a [NIH]

2.10 Isolation of peripheral blood and lamina propria mononuclear cells

Blood from UC patients [$n = 47$] or controls [$n = 9$] was collected and PBMCs were isolated using density gradient centrifugation. LPMCs from intestinal biopsies or gut specimens [$n = 83$] were isolated using the lamina propria kit [Miltenyi Biotec] as previously described.[33] CD4+or CD14+cells were isolated with magnetic beads according to the manufacturer's instructions [Miltenyi Biotec].

2.11 Cell culture

Human or murine LPMCs from gut specimens or biopsies were isolated using the lamina propria kit [Miltenyi Biotec]. Cells were cultivated in RPMI 1640 GlutaMax [Gibco] supplemented with 100 U/mL penicillin/streptavidin [Gibco], 10% FCS [Sigma-Aldrich] and gentamycin [Gibco]. LPMCs were stimulated for 24, 48 or 72 h with 1 µg/mL lipopolysaccharide [LPS; Sigma-Aldrich], 1 µg/mL LPS in combination with 100 µM cobitolimod [InDex Pharmaceuticals], 1 µg/mL LPS and anti-IL10 [abcam] or 1 µg/mL LPS and anti-IL17 [abcam]. Stimulated cells were used for flow cytometry analysis, RNA from stimulated LPMCs was isolated and analysed via qRT-PCR, supernatants were collected and analysed with an enzyme-linked immunosorbent assay [ELISA].

In another setting, PBMCs from buffy coats of healthy donors were isolated and 2×10^6 cells per well were seeded in 400 µL RPMI complete medium. Directly after seeding, cobitolimod or cobitolimod with GpC instead of CpG motif was added so that the final concentration in the well reached 0.1, 1 or 10 µM. Cell supernatants were harvested after 48 h of incubation and were used for cytokine measurement by CBA kits [BD], followed by analysis using FCAP Array software from BD according to the manufacturer's instructions. Isolated splenocytes from wildtype or TLR9 knock-out mice were untreated or treated for 48 h with 1, 10 or 100 µM cobitolimod. Release of IL10 was determined by ELISA.

2.12 *In vitro* generation of macrophages

PBMCs from UC patients were isolated using density gradient centrifugation. CD14+PBMCs were isolated with magnetic beads according to the manufacturer's instructions [Miltenyi Biotec]. In total, 1×10^6 CD14+cells per 24-well were cultured for 8 days either with 100 ng/mL macrophage colony-stimulating factor [M-CSF; R&D], 100 ng/mL LPS and 20 ng/mL IFNγ or in combination with 25 µM cobitolimod to generate pro-inflammatory macrophages. For wound healing macrophages, 1×10^6 CD14+cells per well were cultured for 8 days with either 100 ng/mL M-CSF and 20 ng/mL IL4 or in combination with 25 µM cobitolimod. After 8 days in culture, *in vitro* generated pro-inflammatory and wound healing macrophages were analysed via flow cytometry and qRT-PCR.

2.13 *In vitro* chloroquine assay

PBMCs were isolated from healthy donors using density gradient centrifugation according to standard procedures. Cells were seeded onto a 96-well culture at 5×10^5 cells per well in complete RPMI [cRPMI] supplemented with 25 mg/mL gentamicin, 5 mM L-glutamine, 100 IU/mL penicillin, 100 mg/mL streptomycin, 5 mM Hepes and 10% [v/v] heat-inactivated fetal bovine serum. Cells were pre-incubated for 45 min either with medium alone or with 1, 10 or 50 µg/mL chloroquine at 37°C. Cobitolimod was then diluted with cRPMI and added to the well [100 µM per well]. Cells containing medium alone or cobitolimod alone [without chloroquine pre-incubation] were used as a control. Cells were incubated for 48 h and supernatants were used for cytokine measurements either via Luminex or CBA kits, followed by analysis with FCAP Array software according to the manufacturer's instructions.

2.14 *In vitro* TLR9 binding assay

The interaction between cobitolimod as a CpG-ODN and human TLR9 and their kinetics were studied *in vitro* using the Attana A200 system. The Attana A200 is a dual-channel, continuous-flow system for automated analysis based on the Quartz Crystal Microbalance [QCM] technology. The two sensor channels are referred to as channels A and B, where A is used for monitoring of the molecular interaction and B serves as a reference. Proteoliposomes with TLR9 or protein mock control were immobilized by adsorption on polystyrene [PS] surfaces. A final protein concentration of 250 µg/mL was diluted into PS buffer [5 mM acetic acid pH 5, 50 mM NaCl]. The solution was incubated over the PS surfaces for 3 h at room temperature. Equal volume of liposomes were used to prepare the protein mock control surfaces. The chips were docked in the instrument with the flow set at 100 µL/min for 10 min. After reducing the flow to 20 µL/min, running buffer was passed over the surfaces until stabilization of the baseline [frequency change ≤ 0.2 Hz over 600 s]. Cobitolimod was injected in duplicates at different concentrations: 200, 100, 50 or 25 µg/mL. The experiment was performed at a flow rate of 20 µL/min. Samples were injected for 60 s and the dissociation was followed for 180 s. Sensograms were collected using Attester software [Attana AB] and analysed with Evaluation software [Attana AB] and TraceDrawer [Ridgeview]. The sensograms obtained from channel A were subtracted from the signal obtained from the reference surface in channel B. To calculate the kinetic parameters [k_a and k_d] and affinity constant [K_D], the experimental data were fitted using a 1:1 model. In a 1:1 model, the curve fitting describes the interaction between a

monovalent analyte that binds the target on a single site. The fit generates an association rate constant (k_a [1/M·s]), a dissociation rate constant [k_d [1/s]] and an affinity constant [K_D [M]] calculated as the ratio k_a/k_d.

2.15 Enzyme-linked immunosorbent assay

An ELISA was performed using IFNγ, TNFα, IL1β, IL6, IL17, TGFβ, IL4 and IL10 ELISA kits [eBioscience] according to the manufacturer's instructions.

2.16 Flow cytometry

For different experiments, LPMCs were isolated from intestinal biopsies of mice treated with DSS or from the colon of UC patients and cultured as described above. Prior to intracellular staining, cells were treated with a stimulation cocktail containing phorbol 12-myristate-13-acetate [PMA], Golgi-Stop and Ionomycin [eBioscience] for 4 h at 37°C. Cells were fixed and permeabilized using a transcription factor buffer set [BD Biosciences] according to the manufacturer's instructions. Cells were stained for CD4 [BD Pharmingen], Tbet [Biolegend], IFNγ [BD Pharmingen], GATA3 [BD Pharmingen], IL4 [Biolegend], IL17A [Biolegend], RorγT [BD Pharmingen] and respective isotype controls. For other experiments cells were stained with CD4 [Biolegend], CD8 [Biolegend], CD14 [BD Pharmingen], CD15 [Biolegend], CD19 [BD Pharmingen], CD11c [BD Pharmingen], NK1.1 [Biolegend], CD68 [BD Pharmingen], CD80 [Biolegend], CD163 [Biolegend], CD206 [BD Pharmingen], CD25 [BD Pharmingen], FoxP3 [BD Pharmingen], CD49b [Biolegend], LAG3 [Biolegend] and IL10 [Biolegend]. Flow cytometry analysis was performed with FACS Calibur [BD Biosciences]. Cells were analysed using the FlowJo single cell analysis software [v.10.1r5, TreeStar].

2.17 Statistics

Statistical analysis was performed using Graph Pad Prism [Graph Pad Software]. After testing for normal distribution with the Shapiro–Wilk normality test, significant differences between samples were calculated using the unpaired Student's *t* test or the Mann-Whitney U-rank test [$*p \le 0.05$; $**p \le 0.01$; $***p \le 0.001$].

3. Results

3.1 Intestinal TLR9 expression correlates with severity of inflammation in UC patients and activation of TLR9 leads to heightened IL10 production

To determine TLR9 expression in UC, we performed qPCR analysis of colonic biopsies from UC patients with different levels of histological inflammation. We observed a significant positive correlation between levels of histological inflammation and intestinal TLR9 levels, and highest expression could be demonstrated in UC patients with severe inflammation [Figure 1A]. Histological, endoscopic and clinical assessment scores of UC patients are depicted in Supplementary Table 1. As these findings indicated a possible link between TLR9 signalling and mucosal inflammation in UC, we subsequently studied the molecular effects of the TLR9 agonist cobitolimod. To prove the specific interaction between cobitolimod as a CpG motif containing ODN and human TLR9, we performed an *in vitro* TLR9 binding assay. The respective sensograms showed that cobitolimod specifically binds to TLR9 [Figure 1B]. The calculated kinetics parameters indicated medium-fast association rates [k_a] and fast dissociation rates [k_d]. Strong binding affinity was detected for cobitolimod as revealed by the low affinity constant [K_D] [Supplementary Table 2]. After showing that cobitolimod was able to interact with TLR9 *in vitro*, we next analysed its ability to impact mucosal cytokine production. We therefore stimulated isolated LPMCs from UC patients with different concentrations of cobitolimod *in vitro*. A dose-dependent, significant induction of IL6, TGFβ and IL10 production could be recorded, with IL10 showing the highest observable levels [Figure 1C].

To investigate CpG motif-dependent IL10 production, PBMCs of human controls were treated with either CpG motif-containing cobitolimod or a control ODN of cobitolimod containing a reverse CpG [GpC] motif. It could be shown that only PBMCs that were treated with cobitolimod exhibited significantly elevated IL10 levels, while PBMCs treated with the control ODN failed to induce IL10 production, thus demonstrating the dependency of an intact CpG motif for the induction of IL10 production [Figure 1D]. Moreover, pre-incubation with different concentrations of chloroquine, an endosomal TLR inhibitor, inhibited IL10 release of cobitolimod-treated human PBMCs in a dose-dependent manner [Figure 1E], suggesting that cobitolimod induces IL10 production via TLR signalling.

To further prove the specific ability of cobitolimod to activate IL10 production via the TLR9 pathway, we stimulated splenocytes from wildtype and TLR9 knockout mice with different concentrations of the TLR9 agonist *in vitro*. As expected, cobitolimod induced IL10 production in splenocytes from wildtype mice, whereas the induction of IL10 was absent in TLR9 knockout mice [Figure 1F]. These results underline the ability of cobitolimod to activate the human and murine TLR9 pathways, resulting in heightened mucosal IL10 production.

3.2 Rectal administration of cobitolimod ameliorates DSS-induced colitis in mice

In subsequent studies, we evaluated the *in vivo* effects of cobitolimod in a murine model of intestinal inflammation induced by DSS. Four days after initiation of DSS administration, mice started to lose weight, indicating the presence of active mucosal inflammation. Rectal application of cobitolimod on days 4 and 8 resulted in a significantly reduction of body weight loss compared to placebo-treated mice [Figure 2A]. Analysis of DAI values confirmed that cobitolimod ameliorates DSS-induced colitis.[25,26] Cobitolimod-treated mice demonstrated a reduced DAI compared to placebo-treated mice from day 6 until the end of the experiment [Figure 2B]. In addition, the results of the endoscopic inflammatory score [MEICS score] confirmed the anti-inflammatory effect upon cobitolimod application. All cobitolimod-treated mice developed diminished signs of endoscopic inflammation compared to the placebo-treated group [Figure 2C]. We also observed a significantly reduced histopathological score in cobitolimod-treated animals as compared to placebo-treated mice [Figure 2D]. However, suppression of mucosal inflammation was higher in the 84 and 250 µg dose groups of cobitolimod compared to the 40 µg dose group, indicating a dose-dependent therapeutic efficacy of this drug. In summary, these findings show that rectal cobitolimod administration is able to ameliorate experimental DSS-induced colitis.

3.3 Upregulation of IL10- and downregulation of IL17-dependent mucosal signalling pathways upon cobitolimod treatment in DSS-induced colitis mice

To gain further insights into the effects of cobitolimod on immune cell modulation, we performed microarray analysis of the differentiated gene expression profiles in LPMCs isolated from cobitolimod- or

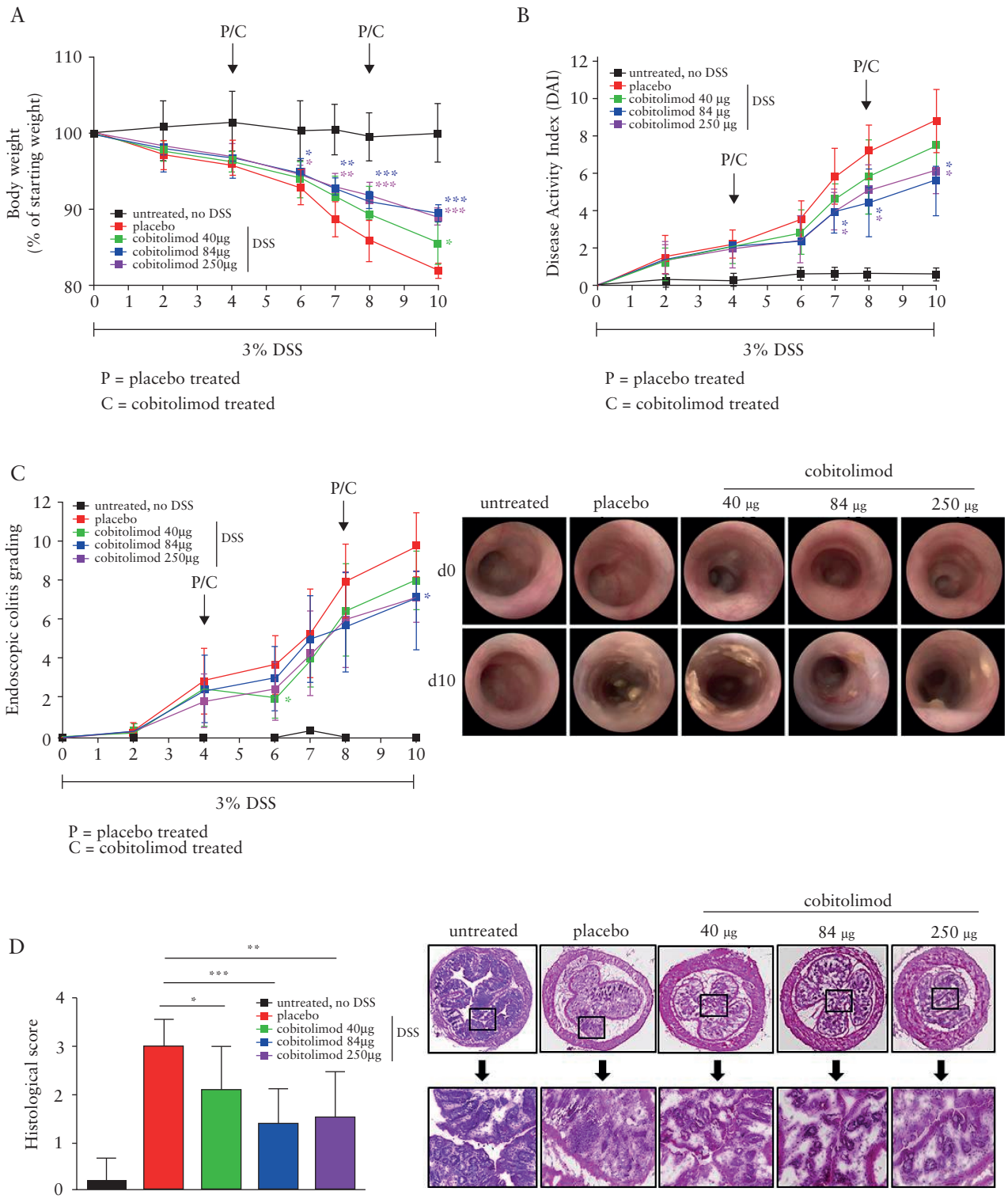

Figure 2. Impact of cobitolimod treatment on clinical, endoscopic and histological disease activity in the experimental mouse model of DSS-induced colitis. 3% DSS was added for 10 days to the drinking water of female Balb/c mice. A control group [no DSS] was also part of the experimental set-up [$n = 3$]. Cobitolimod [40, 84 or 250 µg] or placebo, was rectally administered on days 4 and 8 [$n = 7$ mice per group] to DSS-treated mice. [A] Body weight was monitored on days 0, 2, 4, 6, 7, 8 and 10. [B] Disease activity index [DAI] is the combined score of body weight loss compared to initial body weight, stool consistency and visible blood in faeces. The maximum score per mouse is 12. DAI was assessed on days 0, 2, 4, 6, 7, 8 and 10. [C] Endoscopic colitis grade consists of the following five parameters: thickening of the colon, change of the normal vascular pattern, presence of fibrin, mucosal granularity and stool consistency. Grading [score 0–3] was performed for each parameter leading to a final accumulative score, the endoscopic colitis grading, between 0 and 15. Endoscopic grading was analysed on days 0, 2, 4, 6, 7, 8 and 10 [left panel]. Representative endoscopic examples for day 0 and day 10 for each group are shown [right panel]. [D] Histopathological analysis of intestinal sections. A histological score [0 = no inflammation, 1 = remission, 2 = mild, 3 = moderate, 4 = severe colitis] was used to quantify severity of DSS-induced colitis [left panel] in mice intestinal specimens taken at day 10. Representative intestinal H&E stainings of each group are shown [right panel]. Data represent mean values ± SD. $*p \leq 0.05$; $**p \leq 0.01$; $***p \leq 0.001$ comparing cobitolimod vs placebo-treated animals.

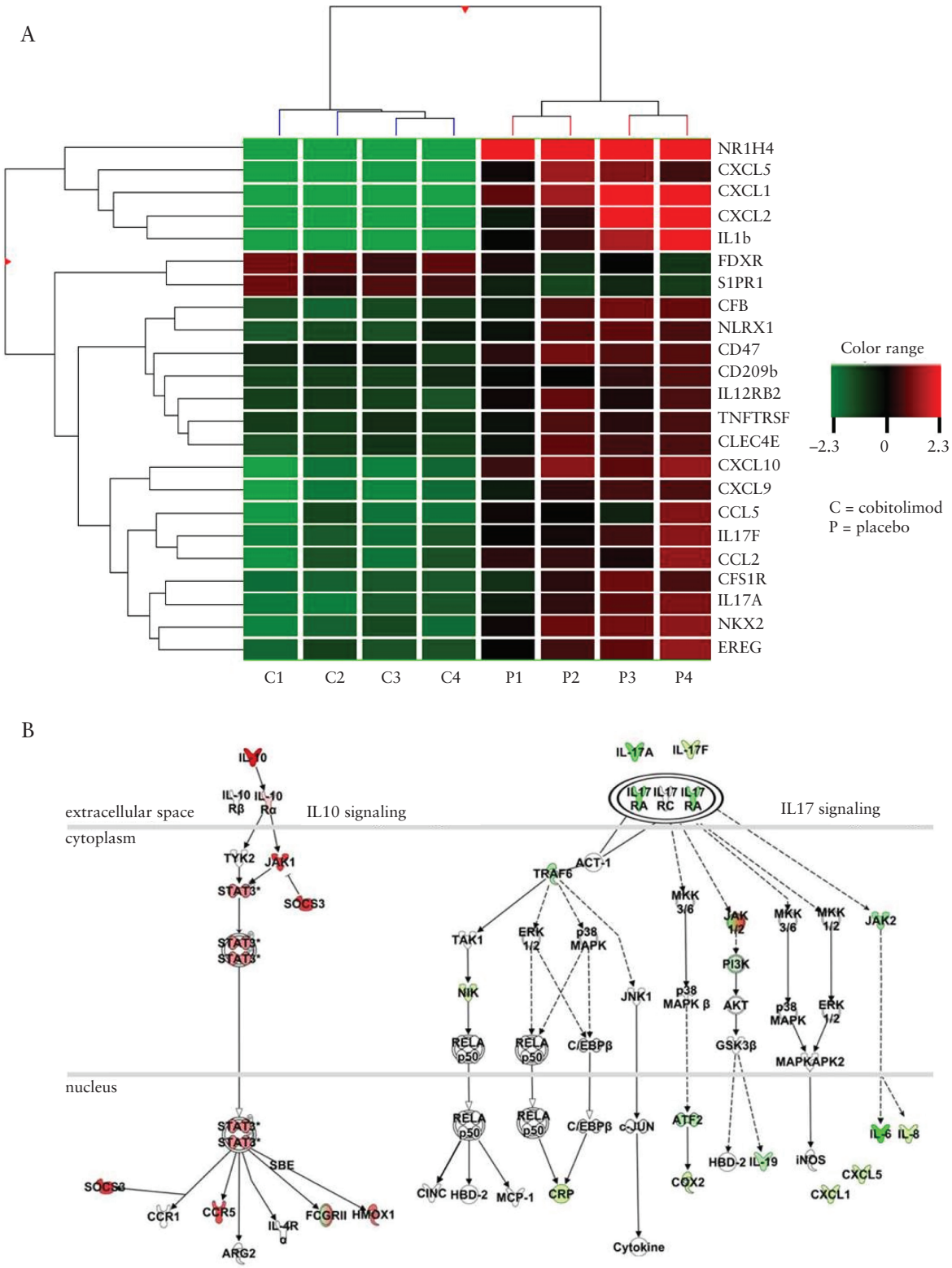

Figure 3. Heatmap of genes showing microarray-based differential expression of DSS-induced colitis susceptibility genes and signalling pathway analysis of IL10- and IL17-dependent genes upon cobitolimod treatment. [A] Gene expression profiles of isolated LPMCs from placebo- [P, $n = 4$] or cobitolimod- [C, $n = 4$] treated DSS colitis mice. Shown as a heat map are expression patterns of 23 DSS-induced colitis susceptibility genes from microarray data, with the corresponding hierarchical clustering of the experimental conditions [placebo or cobitolimod treated mice]. Results were corrected for multiple testing with the Benjamini–Hochberg correction. Pearson and Ward analyses were used to compute hierarchical clustering of the experimental conditions. Expression data for each gene/row were normalized to the median expression value of the respective gene across all eight samples. [B] Ingenuity Pathway Analysis of placebo- or cobitolimod-treated DSS colitis mice showing IL10 and IL17 signalling pathways. The intensity of the colour indicates the level of upregulation [red] or downregulation [green] of respective molecules in cobitolimod- compared to placebo-treated DSS colitis mice.

placebo-treated mice with DSS-induced colitis. There was a significant downregulation of pro-inflammatory genes in cobitolimod- compared to placebo-treated mice [Figure 3A]. Next, Ingenuity Pathway Analysis of the microarray results was performed regarding the IL10 and IL17 signalling pathways. We observed a clear upregulation of the IL10 signalling pathway and a downregulation of the IL17 signalling pathway in cobitolimod- compared to placebo-treated mice [Figure 3B]. These results demonstrate that cobitolimod application in DSS-induced colitis is associated with an impact on the mucosal IL10- and IL17-dependent signalling pathways.

3.4 Cobitolimod significantly decreases mucosal Th17/IL17+cells and increases FoxP3+and IL10+cells in DSS-induced colitis mice

Next, we characterized the underlying mechanisms of the anti-inflammatory effect of cobitolimod in DSS-induced colitis. Accordingly, we performed flow cytometry analysis from LPMCs, which were isolated from colon specimens taken at the end of the DSS-induced colitis experiment on day 10. Interestingly, we observed significantly reduced levels of RorγT+IL17+, RorγT+and IL17+T cells in cobitolimod- compared to placebo-treated mice. However, we did not observe differences in Th1 or Th2 cells and their associated cytokines and transcription factors [T-bet, GATA3] [Figure 4A]. Moreover, colonic specimens taken at the end of the experiment on day 10 showed significantly reduced levels of IL6, IL17F and IL17A mRNA and significantly increased levels of FoxP3 in cobitolimod- compared to placebo-treated mice [Figure 4B]. In this setting we did not observe differences for IL10 mRNA expression levels. These results indicated that cobitolimod might also have an influence on FoxP3+regulatory T cells. To further investigate the role of cobitolimod in the regulation of Th17 and Treg cells, we performed immunofluorescence analysis of colonic biopsies, which were taken at the end of the DSS-induced colitis experiment at day 10. We observed that the number of IL17+cells was significantly decreased [Figure 4C], while the amount of IL10+[Figure 4D] and FoxP3+cells [Figure 4E] was significantly increased in cobitolimod- compared to placebo-treated mice.

3.5 Cobitolimod influences the Th17/Treg immune cell response *in vitro* in UC patients

To confirm our findings from the murine DSS-induced colitis model in humans, we first isolated LPMCs from the colon of UC patients and stimulated them *in vitro* for different time periods with LPS alone, or in combination with cobitolimod. Cobitolimod application led to suppressed mRNA levels of IL6, IL17A and IL17F, whereas IL10 and Foxp3 expression were markedly increased. Only a tendency but no significant differences could be observed for FoxP3 expression after 72 h of *in vitro* stimulation [Figure 5A]. Analysis of the supernatants of the treated LPMCs confirmed that *in vitro* cobitolimod application significantly decreased the production of the pro-inflammatory cytokine IL17 [Figure 5B], while it significantly increased the production of the anti-inflammatory cytokine IL10 in LPMCs from UC patients after 24 and 72 h *in vitro*. We did not observe significant differences after 48 h [Figure 5B].

In functional studies, we next investigated the specificity of cobitolimod-induced downregulation of IL17. We treated isolated LPMCs from UC patients with LPS, LPS and cobitolimod or together in combination with a blocking anti-IL10 antibody and analysed the amount of CD4+IL17+cells via flow cytometry. Cobitolimod decreased the number of CD4+IL17+cells *in vitro*, while the addition of an inhibitory anti-IL10 antibody completely abrogated the downregulatory effect of cobitolimod [Figure 5C]. These results indicate that mucosal upregulation of IL10 upon *in vitro* cobitolimod treatment causes subsequent downregulation of IL17 expression.

3.6 Cobitolimod application induces IL10-producing mucosal wound healing macrophages and Tregs *in vitro* in UC patients

To investigate which cell types are the main producers of IL10 following *in vitro* cobitolimod application, we treated LPMCs and PBMCs of UC patients *in vitro* with LPS or LPS in combination with cobitolimod and analysed IL10 expression via flow cytometry. CD4+T cells and CD14+monocytes/macrophages were the main inducers of IL10 after *in vitro* cobitolimod application in both LPMCs [Figure 6A] and PBMCs [Figure 6B]. In contrast, we did not detect differences in IL10 release in CD8+, CD15+, CD19+, CD11c+or NK1.1+cells [Figure 6A and B]. To further characterize the IL10-producing CD14+macrophages, we next distinguished cobitolimod effects on CD14+CD68+CD80+pro-inflammatory macrophages [‘classical activated M1-like macrophages’] and CD14+CD163+CD206+wound healing macrophages [‘alternatively activated M2-like macrophages’]. The *in vitro* treatment of CD14+PBMCs with cobitolimod resulted in downregulation of pro-inflammatory macrophages [Figure 6C, upper left panel] and also led to diminished expression of the pro-inflammatory cytokine IL12 by these pro-inflammatory macrophages [Figure 6C, lower left panel]. A representative gating strategy for IL12-expressing pro-inflammatory macrophages after application of LPS or LPS with cobitolimod is shown [Figure 6C, right panel]. Moreover, the *in vitro* treatment of CD14+PBMCs from UC patients with cobitolimod caused an upregulation of CD14+CD163+CD206+wound healing macrophages [Figure 6D, upper left panel] and also increased IL10 expression by these cells [Figure 6D, lower left panel]. A representative gating strategy for IL10-expressing wound healing macrophages after application of LPS or LPS with cobitolimod is shown [Figure 6D, right panel]. These data indicate that CD4+T cells and wound healing macrophages are the main producers of IL10 upon cobitolimod administration *in vitro*.

To analyse whether cobitolimod also influences the polarization and differentiation of macrophages, we isolated CD14+cells from PBMCs of UC patients, polarized them to pro-inflammatory or wound healing macrophages and applied cobitolimod *in vitro*. Flow cytometry analysis of *in vitro* generated macrophages revealed that cobitolimod influenced the polarization of these cells. The addition of cobitolimod to the *in vitro* generated macrophages resulted in reduced mean fluorescence intensity [MFI] of CD14+CD68+CD80+pro-inflammatory macrophages [Figure 7A] and elevated MFI levels of CD14+CD163+CD206+wound healing macrophages [Figure 7B] compared to *in vitro* generated macrophages without subsequent stimulation with cobitolimod. qRT-PCR analysis of the mRNA level in these *in vitro* generated macrophages demonstrated that application of cobitolimod results in significantly decreased expression of CD80 [Figure 7C] and increased expression of CD163 and CD206 [Figure 7D]. We next analysed the supernatants of the *in vitro* generated macrophages. Cobitolimod treatment resulted in lower production of IL12 by the *in vitro* generated pro-inflammatory macrophages and higher production of IL10 by the in *vitro* generated wound healing macrophages. These results indicate that cobitolimod influences the polarization of CD14+monocytes towards wound healing macrophages *in vitro* [Figure 7E]. Similar results could be observed in mice [Supplementary

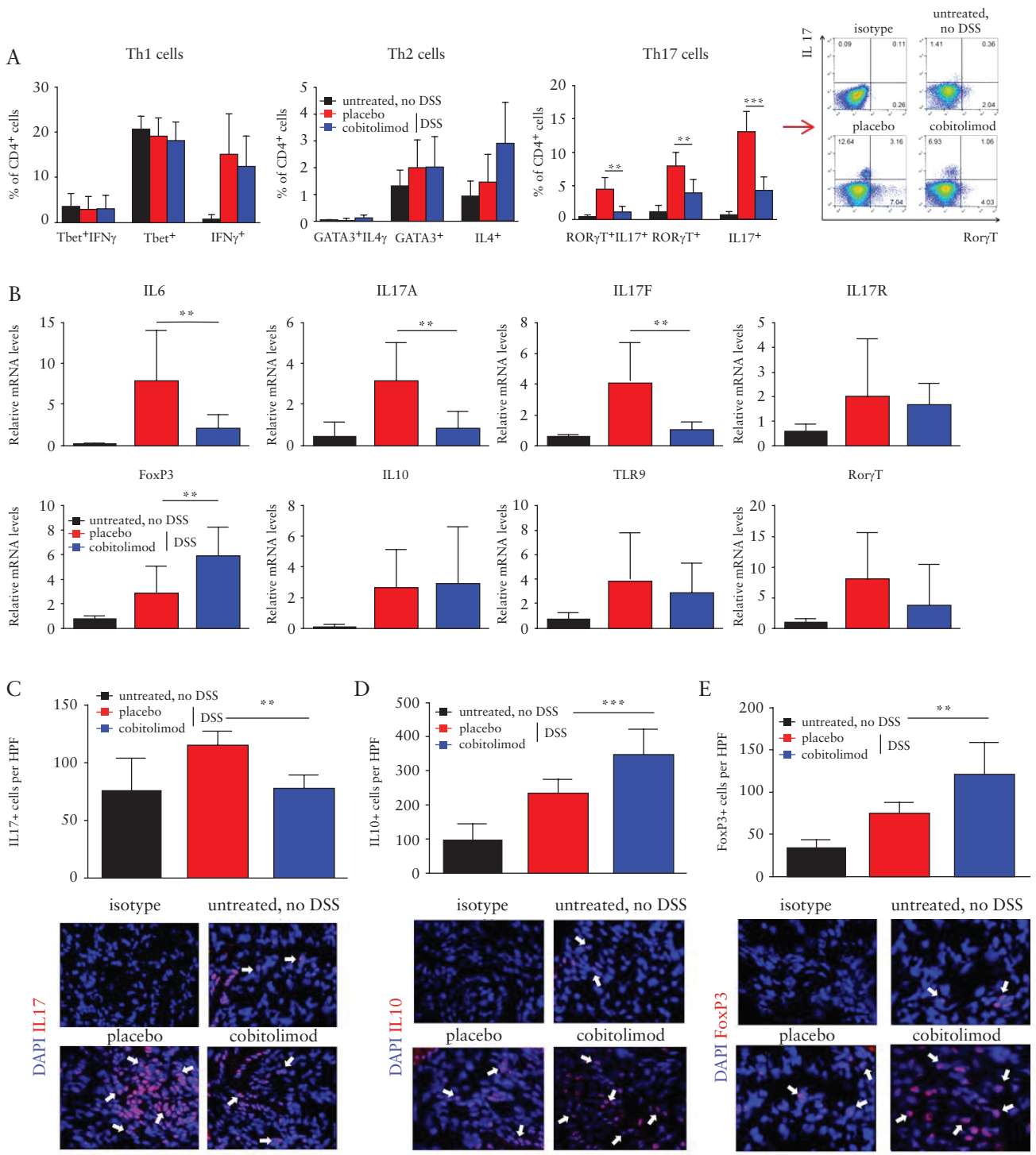

Figure 4. Flow cytometry, qRT-PCR and immunofluorescence analysis of mucosal cells in cobitolimod-treated DSS colitis mice. 3% DSS was added for 10 days to the drinking water of female Balb/c mice. A control group [no DSS] was also part of the experimental set-up [$n = 3$]. Cobitolimod [84 µg] or placebo were rectally applied on days 4 and 8 [$n = 7$ mice per group] to DSS-treated mice. [A] Flow cytometry analysis for Th1, Th2 and Th17 cells from LPMCs isolated from colon specimens taken on day 10 [left panel]. Representative fluorescence-activated cell sorting plot images for Th17 staining of untreated, placebo- or cobitolimod-treated mice [right panel]. [B] qRT-PCR analysis of cytokine expressions from RNA isolated from colon specimens taken on day 10. Data were normalized to the housekeeping gene HPRT. Immunofluorescence analysis of intestinal sections taken on day 10. Mean number and representative immunofluorescence staining of [C] IL17+[left panel], [D] IL10+[middle panel] and [E] FoxP3+cells [right panel]. In all cases, positive cells were counted in five or six high power fields [HPFs] per slide [$n = 7$ mice per group]. Data represent mean values ± SD. *$p \leq 0.01$; **$p \leq 0.01$; ***$p \leq 0.001$.

Figure 1]. We also characterized two distinct CD4+regulatory T cell populations, namely CD4+CD25+Foxp3+classical regulatory T cells and CD4+CD49b+LAG3+FoxP3- type 1 T regulatory [Tr1] cells. We observed that both types of Tregs contribute to the enhancement of IL10-producing cells after cobitolimod application *in vitro* [Supplementary Figure 2].

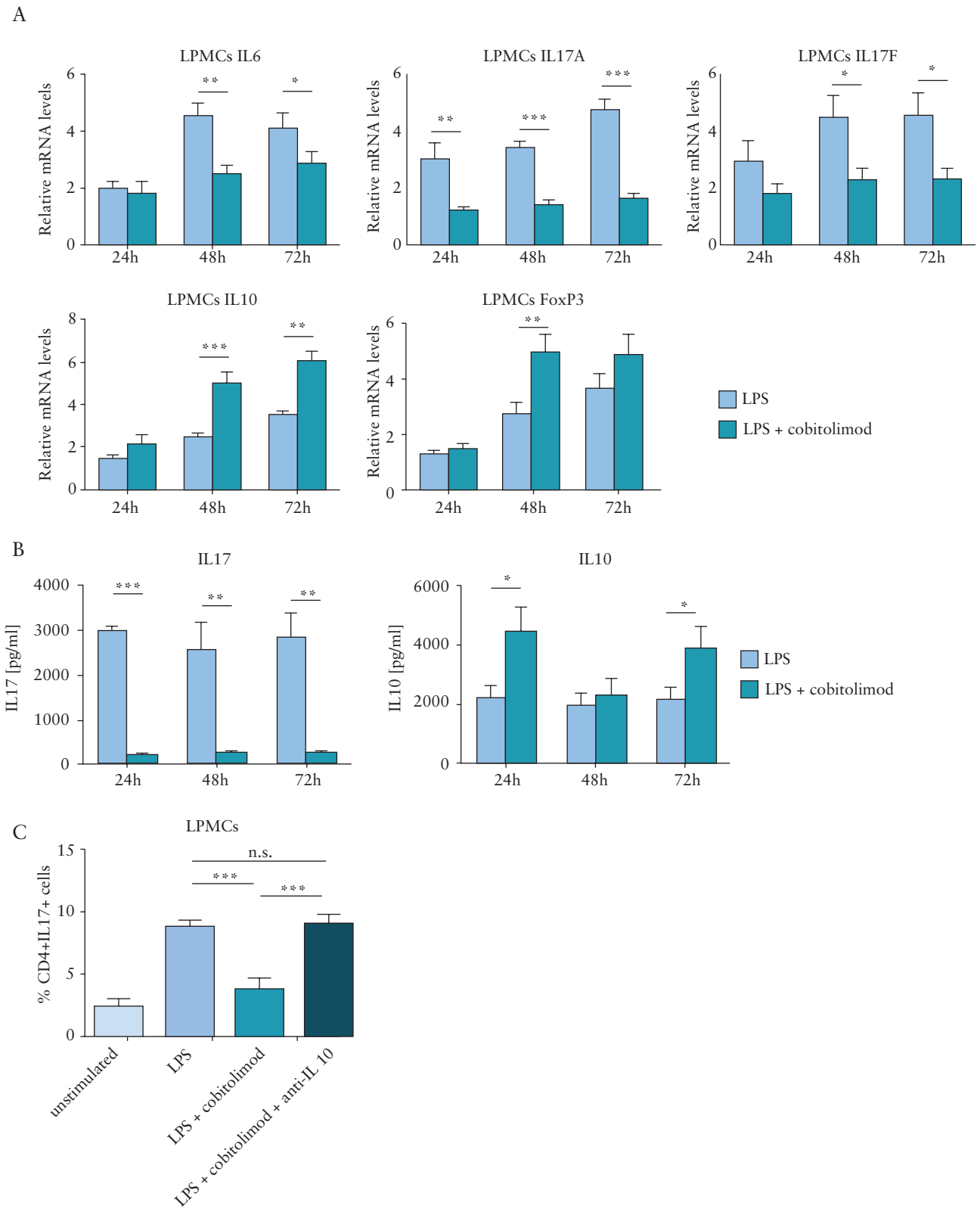

Figure 5. mRNA expression levels and cytokine production of cobitolimod-treated mucosal cells from ulcerative colitis [UC] patients. LPMCs isolated from colon biopsies of UC patients [$n = 10$] were stimulated for 24, 48 or 72 h with LPS [1 µg/mL], or LPS [1 µg/mL] and cobitolimod [100µM]. [A] qRT-PCR was performed to analyse mRNA expression levels of different cytokines or FoxP3. Data were normalized to the housekeeping gene HPRT. [B] Supernatants of stimulated LPMCs were collected and concentrations of total IL17 [left panel] and IL10 [right panel] were determined by ELISA. [C] Isolated LPMCs from colon biopsies of UC patients [$n = 7$] were unstimulated or stimulated for 48 h with LPS, LPS and 100 µM cobitolimod, or LPS and 100 µM cobitolimod and anti-IL10. Expression levels of CD4+IL17+cells were determined via flow cytometry. Data represent mean values ± SD. *$p \leq 0.05$; **$p \leq 0.01$; ***$p \leq 0.001$. n.s.: not significant.

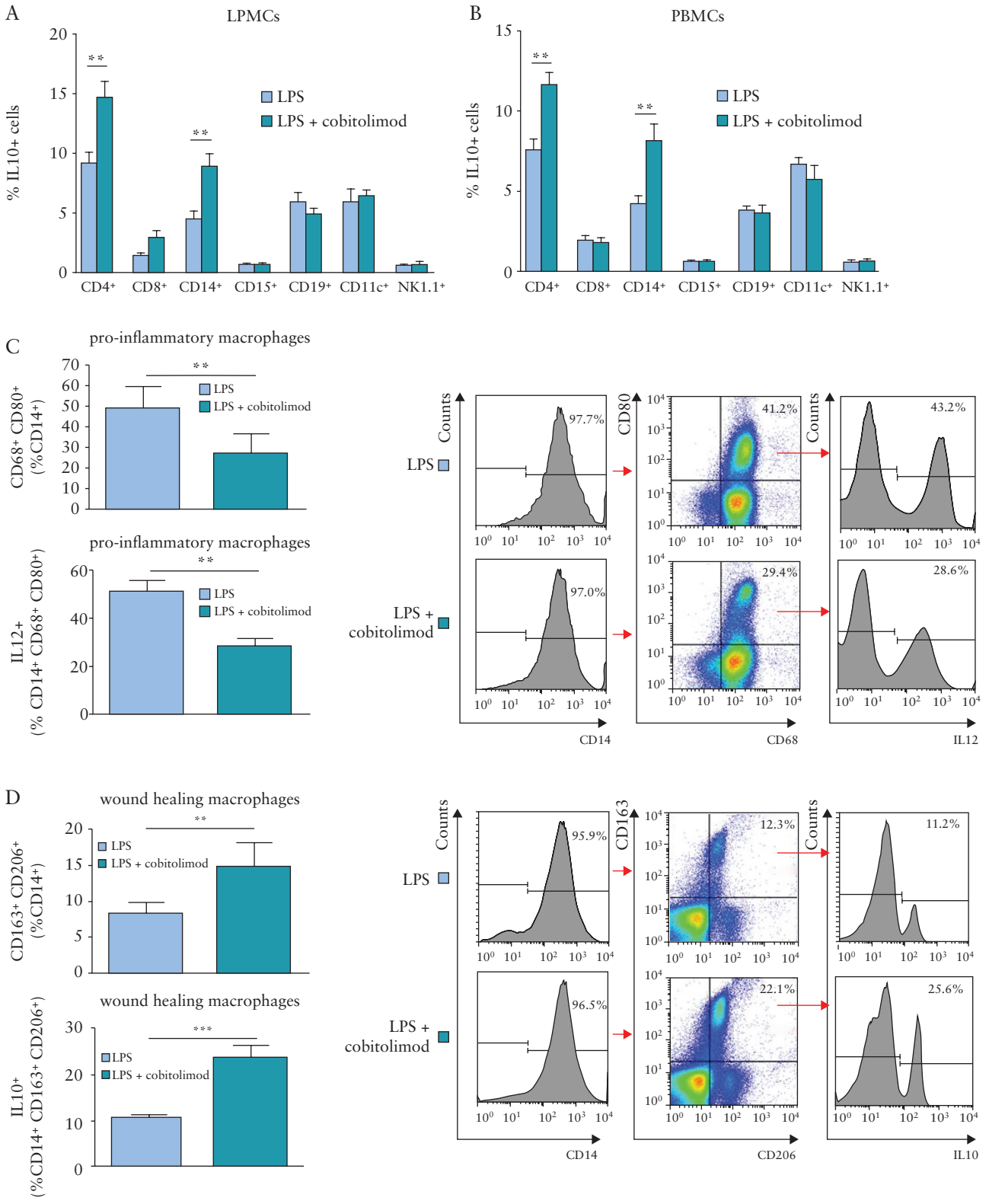

Figure 6. Analysis of IL10-producing cells of ulcerative colitis [UC] patients after *in vitro* application of cobitolimod. [A] Isolated LPMCs from the colon of UC patients [$n = 8$] were stimulated for 48 h with LPS [1 µg/mL] or LPS [1 µg/mL] and cobitolimod [100 µM] after which the percentages of IL10-producing cells of different cell populations [CD4+, CD8+, CD14+, CD15+, CD19+, CD11c+and NK1.1+] were determined via flow cytometry. [B] Isolated PBMCs from UC patients [$n = 8$] were stimulated for 48 h with LPS [1 µg/mL] or LPS [1 µg/mL] and cobitolimod [25 µM]. Expression levels of IL10-producing cells were determined via flow cytometry. [C] CD14+PBMCs from UC patients [$n = 8$] were stimulated for 48 h with LPS [1 µg/mL] or LPS [1 µg/mL] and cobitolimod [25 µM] and IL12-producing pro-inflammatory macrophages were analysed by flow cytometry. CD14+cells were gated and within CD14+cells the percentage of CD68+CD80+cells was determined. IL12-producing cells out of CD14+CD68+CD80+cells were analysed. [D] CD14+PBMCs from UC patients [$n = 8$] were stimulated for 48 h with LPS [1 µg/mL] or LPS [1 µg/mL] and cobitolimod [25 µM] and IL10-producing wound healing macrophages were analysed by flow cytometry. CD14+cells were gated and within CD14+cells the percentage of CD163+CD206+cells was determined. IL10-producing cells out of CD14+CD163+CD206+cells were analysed. Data represent mean values ± SD. $^{**}p \leq 0.01$; $^{***}p \leq 0.001$

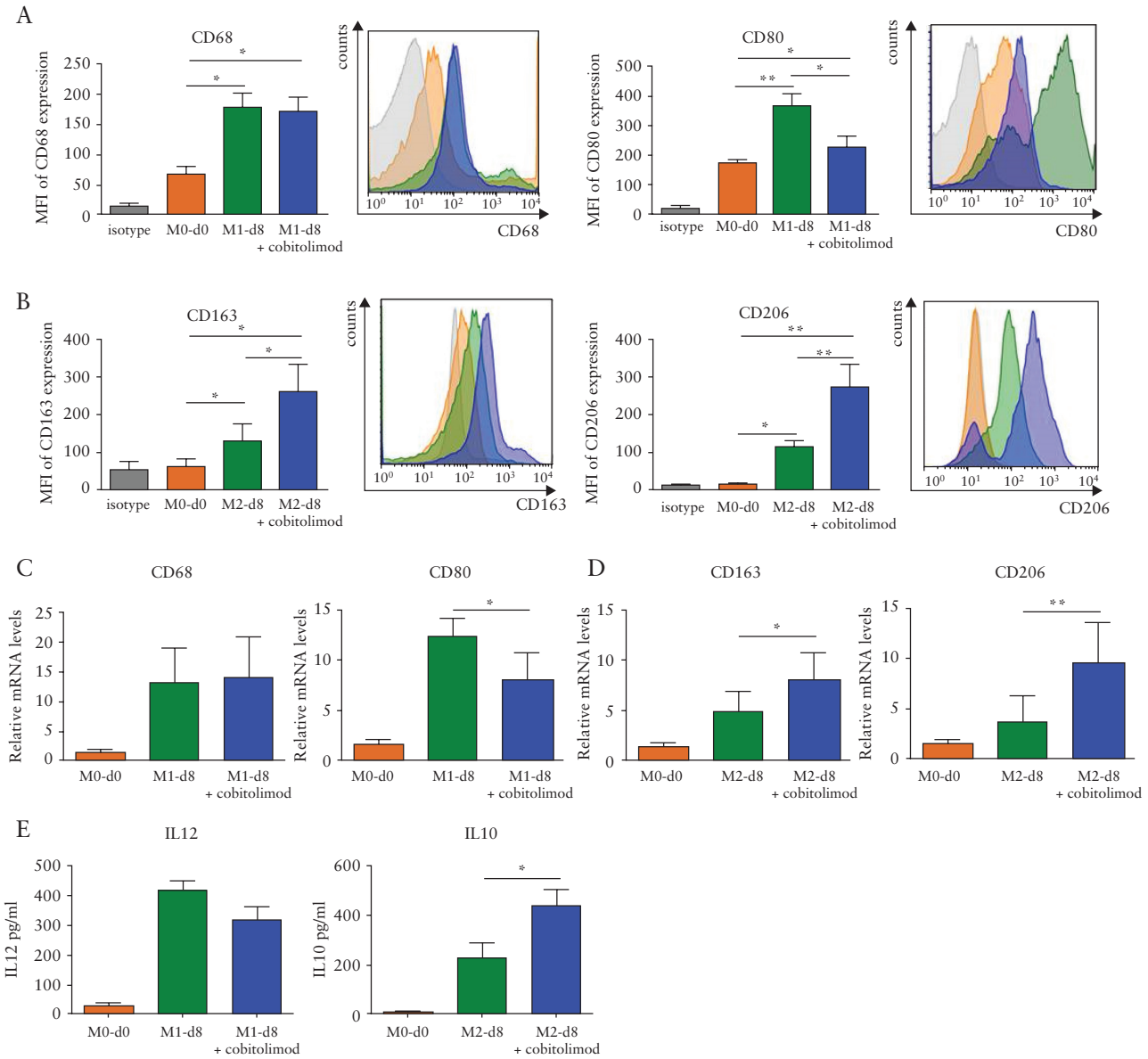

Figure 7. Analysis of *in vitro* generated macrophages from ulcerative colitis [UC] patients after cobitolimod application. CD14+PBMCs ['M0-d0'] from UC patients were cultured for 8 days [d8] either with 100 ng/mL M-CSF, 100 ng/mL LPS and 20 ng/mL IFNγ or in combination with 25 µM cobitolimod to generate pro-inflammatory macrophages ['M1-d8']. CD14+PBMCs ['M0-d0'] were cultured for 8 days [d8] either with 100 ng/mL M-CSF and 20 ng/mL IL4 or in combination with 25 µM cobitolimod to generate wound healing macrophages ['M2-d8']. [A] After 8 days in culture, *in vitro* generated pro-inflammatory macrophages ['M1-d8'] were analysed via flow cytometry. Therefore, CD14+CD80+or CD14+CD68+cells were gated and within the positive cells mean fluorescence intensities of CD68 or CD80 were quantified. Shown are bar graph summaries of averages of mean fluorescence intensities of CD68 [respective left panel] and CD80 [respective left panel] from all UC patients [$n = 9$] and representative histogram overlays from isotype, M0-d0, M1-d8 and M1-d8 plus cobitolimod [respective right panel]. [B] After 8 days in culture, *in vitro* generated wound healing macrophages ['M2-d8'] were analysed via flow cytometry. Therefore, CD14+CD206+or CD14+CD163+cells were gated and within the positive cells mean fluorescence intensities of CD163 or CD206 were quantified. Shown are bar graph summaries of averages of mean fluorescence intensities of CD163 [respective left panel] and CD206 [respective left panel] from all UC patients [$n = 9$] and representative histogram overlays from isotype, M0-d0, M2-d8 and M2-d8 plus cobitolimod [respective right panel]. [C] qRT-PCR was performed to analyse mRNA expression levels of CD68 and CD80 from *in vitro* generated pro-inflammatory macrophages. Data were normalized to the housekeeping gene HPRT [D] qRT-PCR was performed to analyse mRNA expression levels of CD163 and CD206 from *in vitro* generated wound healing macrophages. [E] IL12 ELISA was performed in the supernatants of *in vitro* generated pro-inflammatory macrophages [left panel] and IL10 ELISA was performed with the supernatants of *in vitro* generated wound healing macrophages [right panel]. Data represent mean values ± SD. $*p \leq 0.05$; $**p \leq 0.01$.

3.7 Readjusting the Th17/Treg balance in UC patients responding to cobitolimod therapy

Finally, we investigated the presence of IL17, FoxP3 and IL10 in colon biopsy sections obtained from UC patients before [screening] and after [week 4] application of cobitolimod [responder and non-responder] or placebo in a controlled clinical trial. IL17+mucosal cells were significantly reduced [Figure 8A], whereas IL10+[Figure 8B] and FoxP3+[Figure 8C] cells were significantly increased in the colon of cobitolimod-treated UC patients that showed clinical and endoscopic signs of response at week 4 as compared to the screening time point [responder]. In contrast, there were no significant differences between weeks 0 and 4 for placebo-treated UC patients and

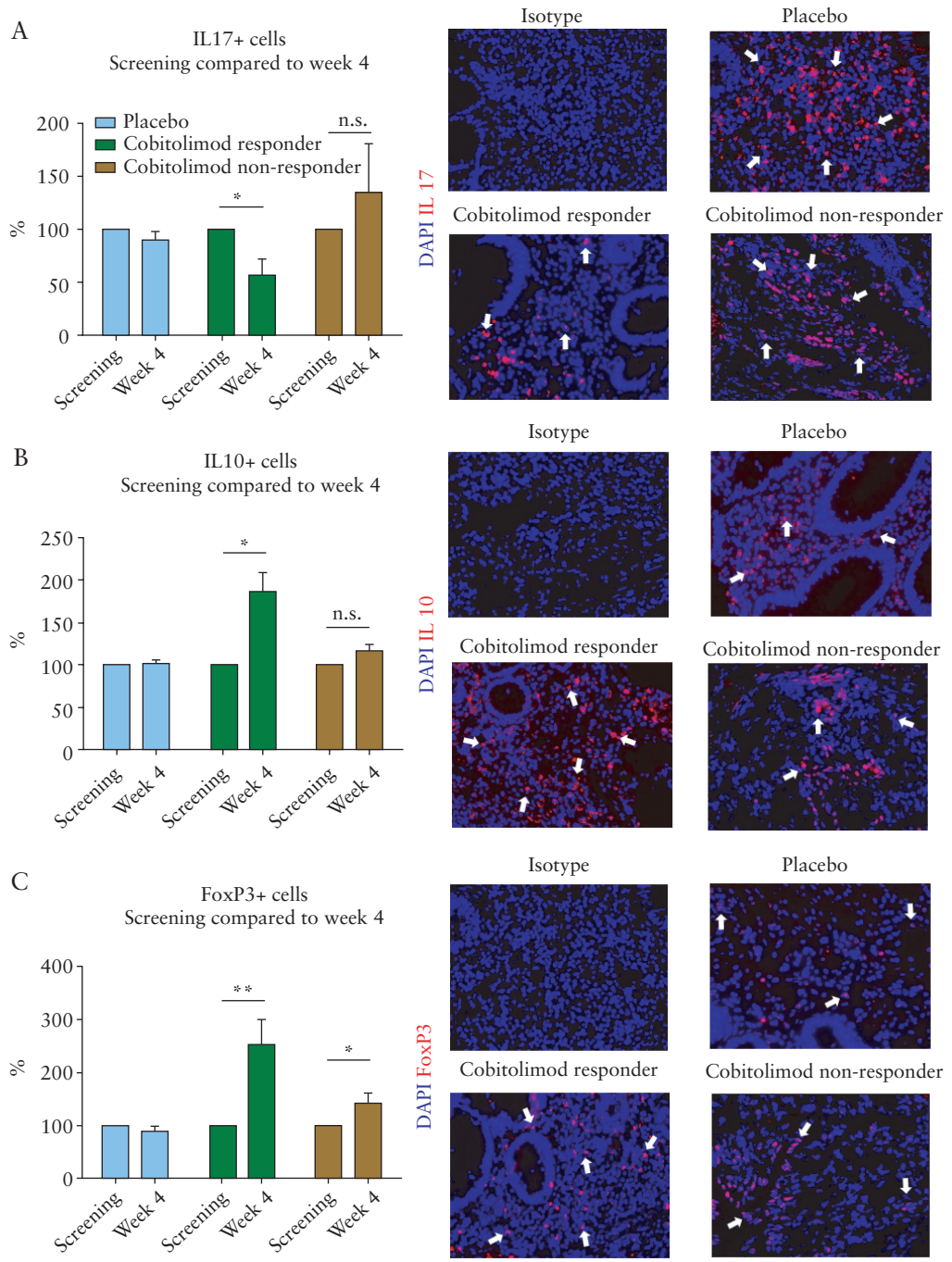

Figure 8. Mucosal immunofluorescence cell analysis of cobitolimod-treated ulcerative colitis [UC] patients. Expression of IL17, IL10 and FoxP3 in colon biopsy sections obtained from UC patients before [screening] and after [week 4] topical treatment with 30 mg cobitolimod [shown are results for cobitolimod responders and non-responders] or placebo. [A] Statistical analyses of IL17+[left panel] cells [placebo $n = 3$; cobitolimod responder $n = 5$; cobitolimod non-responder $n = 6$] and representative immunofluorescence staining of IL17 [right panel]. [B] Statistical analyses of IL10+cells [left panel] [placebo $n = 4$; responder $n = 5$; cobitolimod non-responder $n = 6$] and representative immunofluorescence staining of IL10 [right panel]. [C] Statistical analyses of FoxP3+cells [left panel] [placebo $n = 4$; responder $n = 7$; cobitolimod non- responder $n = 4$] and representative immunofluorescence staining of FoxP3 [right panel]. Positive cells were counted in five or six high-power fields (HPFs) per slide. White arrows indicate positive cells. Data represent mean values ± SD. $^{*}p \leq 0.05$; $^{**}p \leq 0.01$.

cobitolimod-treated UC patients who did not show clinical and endoscopic signs of response at week 4 as compared to the screening time point [non-responder]. Only for FoxP3, also the non-responders showed a significant difference between screening and week 4 but the increase of FoxP3 was more pronounced in responders to cobitolimod therapy. These results indicate that the TLR9 agonist cobitolimod modulates the intestinal immune system in UC patients responding to cobitolimod by modifying the dysregulated Th17/Treg cell response.

4. Discussion

The TLR9 agonist cobitolimod represents a potentially novel therapeutic approach in the treatment of therapy-refractory UC patients

and has shown promising therapeutic effects in early clinical trials.[20–22] However, its exact mechanism of action has not yet been defined. In this study, we characterized the underlying immunomodulatory effects upon cobitolimod application. Our findings demonstrate that cobitolimod modulates the Th17/Treg cell immune imbalance in intestinal inflammation and drives IL10 production by macrophages and T cells, thereby defining a unique mechanism of action for this drug that may be beneficial for UC therapy.

We first found a correlation between intestinal TLR9 expression and severity of inflammation in UC patients, which is in line with previous observations.[14,34] In this study, we tested the immunomodulatory effect of the TLR9 agonist cobitolimod in an experimental DSS colitis mouse model and showed that rectal application of cobitolimod influences the IL10 and IL17 pathway and thereby ameliorates mucosal inflammation in treated mice. It were able to shown that IL10 signalling in Tregs is required for suppression of Th17 cell-mediated inflammation.[35,36] Immunhistochemical analysis revealed significant increases of IL10+and FoxP3+mucosal cells and, by contrast, a significant decrease of IL17+cells in cobitolimod- compared to placebo-treated mice, which in regard to IL17 was also confirmed by flow cytometry and qRT-PCR analysis. We observed differences regarding IL10 mRNA gene expression [Figure 4B] and protein levels [Figure 4C] after cobitolimod application. We observed increased IL10 expression of cobitolimod-treated mice on the protein level, but not on the mRNA gene expression level. It has previously been shown that the degree of correlation between gene expression and protein levels varies across different cytokines and experimental settings.[37] From our point of view, IL10 expression on a protein level is more relevant in the examination and interpretation of cell function. To confirm our findings from the murine DSS-induced colitis model, we performed *in vitro* stimulation experiments with LPMCs from UC patients. Interestingly, we observed that cobitolimod also influences the Th17/Treg cell response in LPMCs from UC patients, as demonstrated by a significant upregulation of IL10 and FoxP3 and a significant downregulation of IL6, IL17A and IL17F *in vitro*. Moreover, addition of a blocking anti-IL10 antibody completely abrogated IL17 downregulation by cobitolimod, indicating that cobitolimod-induced upregulation of IL10 leads to downregulation of IL17. These findings indicate that the suppression of colitis activity by cobitolimod is at least partially due to the induction of IL10 production. The relevance of IL10 in chronic intestinal inflammation is well documented, as IL10- and IL10R-deficient mice have been shown to develop spontaneous chronic colitis.[38–40] Moreover, IL10-producing T regulatory type 1 cells and Tregs are essential for amelioration of experimental colitis and inhibit gut inflammation by CX3CR1+macrophages and T cells.[41,42] Finally, genetic studies in humans have revealed that mutations in *IL10* and *IL10R* genes may cause monogenic forms of IBD.[43,44]

We observed that CD4+and CD14+cells are the main producers of IL10 after cobitolimod treatment of LPMCs or PBMCs from UC patients. Depending on the surrounding environment, macrophage differentiation can lead to the development of M1-like macrophages secreting pro-inflammatory cytokines such as IL12, IL23 or TNFα or of alternatively activated M2-like macrophages, characterized by producing anti-inflammatory mediators such as IL10 or TGFβ.[45,46] M1-like macrophages have been shown to contribute to active inflammation, whereas M2-like wound healing macrophages are deemed important for tissue remodelling, homeostasis and wound healing.[47,48] To further characterize the IL10-producing CD14+monocytes/macrophages after cobitolimod stimulation, we distinguished between CD14+CD68+CD80+pro-inflammatory macrophages and CD14+CD163+CD206+wound healing macrophages. The addition of cobitolimod to the culture of *in vitro* generated macrophages resulted in reduced levels of IL12-producing CD14+CD68+CD80+pro-inflammatory macrophages and elevated levels of IL10-producing CD14+CD163+CD206+wound healing macrophages, compared to *in vitro* generated macrophages without subsequent treatment with cobitolimod. Recently published data suggest that CpG and R848 may drive the macrophages to an M2-like state [IL12lo/IL10hi] in the later phase of activation.[49] Several models have demonstrated that TLR9 ligands may switch macrophages into an 'M2-like' phenotype.[50–52] Our experiments suggest that the TLR9 agonist cobitolimod influences the polarization and differentiation towards IL10-producing, wound healing macrophages. We observed that not only macrophages, but also Tregs, are the main producers of IL10 after cobitolimod treatment. Several studies have reported that expanded Tregs have the capacity to induce phenotypic and functional changes in monocytes and can drive monocytes toward an alternatively activated state.[53–55] Our findings demonstrate that there might be an interaction between induced mucosal Tregs and macrophages after cobitolimod treatment.

Two distinct CD4+Treg populations, Foxp3+Tregs and Foxp3- T regulatory type 1 cells [Tr1], suppress colitogenic T cell responses through the production of IL10 and trigger the anti-inflammatory macrophage phenotype.[56,57] Our data suggest that both types of Tregs contribute via high production of IL10 to the immunomodulatory effect of cobitolimod. It has previously been shown that Tr1 cells cannot express FoxP3 constitutively, but following activation, they upregulate FoxP3 expression to levels such as those expressed in activated T cells. A different study demonstrated that inhibition of FoxP3 expression leads to Tr1 conversion to a Th2-like phenotype and loss of suppressive function, indicating that a conditional microenvironment is a decisive factor for the function and behaviour of Tregs.[58–60] Thus, further analysis needs to be done to distinguish which types of regulatory T cells contribute to the immunomodulatory effect of cobitolimod.

We also investigated the presence of IL17, FoxP3 and IL10 in colon biopsy sections obtained from UC patients with UC before and 4 weeks after topical treatment with cobitolimod or placebo. IL17+cells were significantly decreased, whereas IL10+and FoxP3+cells were significantly increased in the colon of cobitolimod responders. These findings confirm the immunomodulatory effect of cobitolimod. Together, our results from *in vivo* and *in vitro* studies in both humans and mice have shown that cobitolimod treatment decreases the number of Th17 cells and increases Tregs producing IL10, thus correcting the Th17/Treg imbalance. Moreover, there is induction of IL10-producing wound healing macrophages. In conclusion, the TLR9 agonist cobitolimod emerges as a key regulator of IL10-producing macrophages and T cells in the mucosa of UC patients. The immunomodulatory effect of cobitolimod provides a unique novel therapeutic approach in UC and warrants further clinical testing.

Funding

This work was supported in part by grants from InDex Pharmaceuticals AB. CRC1181 Project C02 [RA] and DFG-SFB/TRR241 Project No. C02 [RA] are funded by the German Research Council [DFG]. The DFG funds the Heisenberg Professorship of RA.

Conflict of Interests

RA and MFN report personal fees from InDex Pharmaceuticals AB for advisory work.

Acknowledgements

The authors thank L. Sologub, I. Zöller-Utz, R. SpiegI, A. Böhm, F. Stütz, G. Göhring-Waldeck and Andrea Schneider for excellent technical assistance. We thank the endoscopy unit at the First Department of Medicine, University of Erlangen-Nürnberg, for providing us with samples required to conduct this study. We are indebted to our patients for their participation.

Author Contributions

HS, JU, UB, MV, PS, SS, SR, IA, TR, SZ, ML, JS, AH, TH, CA, TK, CDJ, AZ, MFN and RA provided reagents, protocols, samples or designed experiments; HS, JU, UB, PS and SS performed experiments; HS, MFN and RA designed the study, analysed, discussed, interpreted the data and wrote the manuscript; MFN and RA directed the work.

Supplementary Data

Supplementary data are available at *ECCO-JCC* online.

Podcast

This article has an associated podcast which can be accessed at https://academic.oup.com/ecco-jcc/pages/podcast

References

1. Danese S, Fiocchi C. Ulcerative colitis. *N Engl J Med* 2011;**365**:1713–25.
2. Neurath MF. Cytokines in inflammatory bowel disease. *Nat Rev Immunol* 2014;**14**:329–42.
3. Ford AC, Sandborn WJ, Khan KJ, Hanauer SB, Talley NJ, Moayyedi P. Efficacy of biological therapies in inflammatory bowel disease: systematic review and meta-analysis. *Am J Gastroenterol* 2011;**106**:644–59, quiz 660.
4. Cario E. Therapeutic impact of toll-like receptors on inflammatory bowel diseases: a multiple-edged sword. *Inflamm Bowel Dis* 2008;**14**:411–21.
5. Corridoni D, Chapman T, Ambrose T, Simmons A. Emerging mechanisms of innate immunity and their translational potential in inflammatory bowel disease. *Front Med [Lausanne]* 2018;**5**:32.
6. Cario E. Toll-like receptors in inflammatory bowel diseases: a decade later. *Inflamm Bowel Dis* 2010;**16**:1583–97.
7. Abreu MT. Toll-like receptor signalling in the intestinal epithelium: how bacterial recognition shapes intestinal function. *Nat Rev Immunol* 2010;**10**:131–44.
8. Lee J, Mo JH, Katakura K, *et al*. Maintenance of colonic homeostasis by distinctive apical TLR9 signalling in intestinal epithelial cells. *Nat Cell Biol* 2006;**8**:1327–36.
9. Rose WA 2nd, Sakamoto K, Leifer CA. TLR9 is important for protection against intestinal damage and for intestinal repair. *Sci Rep* 2012;**2**:574.
10. O'Hara JR, Feener TD, Fischer CD, Buret AG. *Campylobacter jejuni* disrupts protective Toll-like receptor 9 signaling in colonic epithelial cells and increases the severity of dextran sulfate sodium-induced colitis in mice. *Infect Immun* 2012;**80**:1563–71.
11. Obermeier F, Strauch UG, Dunger N, *et al*. In vivo CpG DNA/toll-like receptor 9 interaction induces regulatory properties in CD4+CD62L+T cells which prevent intestinal inflammation in the SCID transfer model of colitis. *Gut* 2005;**54**:1428–36.
12. Rachmilewitz D, Karmeli F, Shteingart S, Lee J, Takabayashi K, Raz E. Immunostimulatory oligonucleotides inhibit colonic proinflammatory cytokine production in ulcerative colitis. *Inflamm Bowel Dis* 2006;**12**:339–45.
13. Baumann CL, Aspalter IM, Sharif O, *et al*. CD14 is a coreceptor of Toll-like receptors 7 and 9. *J Exp Med* 2010;**207**:2689–701.
14. Sánchez-Muñoz F, Fonseca-Camarillo GC, Villeda-Ramirez MA, *et al*. TLR9 mRNA expression is upregulated in patients with active ulcerative colitis. *Inflamm Bowel Dis* 2010;**16**:1267–8.
15. Obermeier F, Dunger N, Strauch UG, *et al*. CpG motifs of bacterial DNA essentially contribute to the perpetuation of chronic intestinal inflammation. *Gastroenterology* 2005;**129**:913–27.
16. Fantini MC, Monteleone G. Update on the therapeutic efficacy of tregs in IBD: thumbs up or thumbs down? *Inflamm Bowel Dis* 2017;**23**:1682–8.
17. Gong Y, Liu L, He X, *et al*. The th17/treg immune balance in ulcerative colitis patients with two different chinese syndromes: dampness-heat in large intestine and spleen and kidney yang deficiency syndrome. *Evid Based Complement Alternat Med* 2015;**2015**:264317.
18. Nielsen OH, Kirman I, Rüdiger N, Hendel J, Vainer B. Upregulation of interleukin-12 and -17 in active inflammatory bowel disease. *Scand J Gastroenterol* 2003;**38**:180–5.
19. Gong Y, Lin Y, Zhao N, *et al*. The Th17/Treg immune imbalance in ulcerative colitis disease in a chinese han population. *Mediators Inflamm* 2016;**2016**:7089137.
20. Kuznetsov NV, Zargari A, Gielen AW, *et al*. Biomarkers can predict potential clinical responders to DIMS0150 a toll-like receptor 9 agonist in ulcerative colitis patients. *BMC Gastroenterol* 2014;**14**:79.
21. Atreya R, Bloom S, Scaldaferri F, *et al*. Clinical effects of a topically applied toll-like receptor 9 agonist in active moderate-to-severe ulcerative colitis. *J Crohns Colitis* 2016;**10**:1294–302.
22. Atreya R, Reinisch W, Peyrin-Biroulet L, *et al*. Clinical efficacy of the Toll-like receptor 9 agonist cobitolimod using patient-reported-outcomes defined clinical endpoints in patients with ulcerative colitis. *Dig Liver Dis* 2018;**50**:1019–29.
23. Rutgeerts P, Sandborn WJ, Feagan BG, *et al*. Infliximab for induction and maintenance therapy for ulcerative colitis. *N Engl J Med* 2005;**353**:2462–76.
24. Schroeder KW, Tremaine WJ, Ilstrup DM. Coated oral 5-aminosalicylic acid therapy for mildly to moderately active ulcerative colitis. A randomized study. *N Engl J Med* 1987;**317**:1625–9.
25. Pandurangan AK, Mohebali N, Norhaizan ME, Looi CY. Gallic acid attenuates dextran sulfate sodium-induced experimental colitis in BALB/c mice. *Drug Des Devel Ther* 2015;**9**:3923–34.
26. Ito R, Shin-Ya M, Kishida T, *et al*. Interferon-gamma is causatively involved in experimental inflammatory bowel disease in mice. *Clin Exp Immunol* 2006;**146**:330–8.
27. Becker C, Fantini MC, Wirtz S, *et al*. In vivo imaging of colitis and colon cancer development in mice using high resolution chromoendoscopy. *Gut* 2005;**54**:950–4.
28. Riley SA, Mani V, Goodman MJ, Dutt S, Herd ME. Microscopic activity in ulcerative colitis: what does it mean? *Gut* 1991;**32**:174–8.
29. Ferreira SJ, Senning M, Sonnewald S, Kessling PM, Goldstein R, Sonnewald U. Comparative transcriptome analysis coupled to X-ray CT reveals sucrose supply and growth velocity as major determinants of potato tuber starch biosynthesis. *BMC Genomics* 2010;**11**:93.
30. te Velde AA, de Kort F, Sterrenburg E, *et al*. Comparative analysis of colonic gene expression of three experimental colitis models mimicking inflammatory bowel disease. *Inflamm Bowel Dis* 2007;**13**:325–30.
31. Hansen JJ, Holt L, Sartor RB. Gene expression patterns in experimental colitis in IL-10-deficient mice. *Inflamm Bowel Dis* 2009;**15**:890–9.
32. Breynaert C, Dresselaers T, Perrier C, *et al*. Unique gene expression and MR T2 relaxometry patterns define chronic murine dextran sodium sulphate colitis as a model for connective tissue changes in human Crohn's disease. *PLoS One* 2013;**8**:e68876.
33. Atreya R, Zimmer M, Bartsch B, *et al*. Antibodies against tumor necrosis factor (TNF) induce T-cell apoptosis in patients with inflammatory bowel diseases via TNF receptor 2 and intestinal CD14+macrophages. *Gastroenterology* 2011;**141**:2026–38.
34. Fan Y, Liu B. Expression of Toll-like receptors in the mucosa of patients with ulcerative colitis. *Exp Ther Med* 2015;**9**:1455–9.
35. Chaudhry A, Samstein RM, Treuting P, *et al*. Interleukin-10 signaling in regulatory T cells is required for suppression of Th17 cell-mediated inflammation. *Immunity* 2011;**34**:566–78.

36. Gu Y, Yang J, Ouyang X, *et al*. Interleukin 10 suppresses Th17 cytokines secreted by macrophages and T cells. *Eur J Immunol* 2008;**38**:1807–13.
37. Shebl FM, Pinto LA, García-Piñeres A, *et al*. Comparison of mRNA and protein measures of cytokines following vaccination with human papillomavirus-16 L1 virus-like particles. *Cancer Epidemiol Biomarkers Prev* 2010;**19**:978–81.
38. Kuhn R, Lohler J, Rennick D, Rajewsky K, Muller W. Interleukin-10-deficient mice develop chronic enterocolitis. *Cell* 1993;**75**:263–74.29. Omenetti S, Pizarro TT. The Treg/Th17 axis: a dynamic balance regulated by the gut microbiome. *Front Immuno*l 2015;6:639.
39. Kiesler P, Fuss IJ, Strober W. Experimental models of inflammatory bowel diseases. *Cell Mol Gastroenterol Hepatol* 2015;**1**:154–70.
40. Shouval DS, Biswas A, Goettel JA, *et al*. Interleukin-10 receptor signaling in innate immune cells regulates mucosal immune tolerance and anti-inflammatory macrophage function. *Immunity* 2014;**40**:706–19.
41. Uhlig HH, Coombes J, Mottet C, *et al*. Characterization of Foxp3+CD4+CD25+and IL-10-secreting CD4+CD25+T cells during cure of colitis. *J Immunol* 2006;**177**:5852–60.
42. Zigmond E, Bernshtein B, Friedlander G, *et al*. Macrophage-restricted interleukin-10 receptor deficiency, but not IL-10 deficiency, causes severe spontaneous colitis. *Immunity* 2014;**40**:720–33.
43. Engelhardt KR, Shah N, Faizura-Yeop I, *et al*. Clinical outcome in IL-10- and IL-10 receptor-deficient patients with or without hematopoietic stem cell transplantation. *J Allergy Clin Immunol* 2013;**131**:825–30.
44. Uhlig HH, Powrie F. Translating immunology into therapeutic concepts for inflammatory bowel disease. *Annu Rev Immunol* 2018;**36**:755–81.
45. Kim SY, Nair MG. Macrophages in wound healing: activation and plasticity. *Immunol Cell Biol* 2019;**97**:258–67.
46. Italiani P, Boraschi D. From monocytes to M1/M2 macrophages: phenotypical vs. functional differentiation. *Front Immunol* 2014;**5**:514.
47. Murray PJ, Wynn TA. Protective and pathogenic functions of macrophage subsets. *Nat Rev Immunol* 2011;**11**:723–37.
48. Xue J, Schmidt SV, Sander J, *et al*. Transcriptome-based network analysis reveals a spectrum model of human macrophage activation. *Immunity* 2014;**40**:274–88.
49. Celhar T, Pereira-Lopes S, Thornhill SI, *et al*. TLR7 and TLR9 ligands regulate antigen presentation by macrophages. *Int Immunol* 2016;**28**:223–32.
50. Hanke ML, Angle A, Kielian T. MyD88-dependent signaling influences fibrosis and alternative macrophage activation during *Staphylococcus aureus* biofilm infection. *PLoS One* 2012;7:e42476.
51. Ma C, Ouyang Q, Huang Z, *et al*. Toll-like receptor 9 inactivation alleviated atherosclerotic progression and inhibited macrophage polarized to M1 phenotype in ApoE-/- mice. *Dis Markers* 2015;**2015**:909572.
52. Ferrante CJ, Leibovich SJ. Regulation of macrophage polarization and wound healing. *Adv Wound Care [New Rochelle]* 2012;**1**:10–6.
53. Romano M, Fanelli G, Tan N, *et al*. Expanded regulatory T cells induce alternatively activated monocytes with a reduced capacity to expand T helper-17 cells. *Front Immunol* 2018;**9**:1625.
54. Tiemessen MM, Jagger AL, Evans HG, van Herwijnen MJ, John S, Taams LS. CD4+CD25+Foxp3+regulatory T cells induce alternative activation of human monocytes/macrophages. *Proc Natl Acad Sci U S A* 2007;**104**:19446–51.
55. Sun W, Wei FQ, Li WJ, *et al*. A positive-feedback loop between tumour infiltrating activated Treg cells and type 2-skewed macrophages is essential for progression of laryngeal squamous cell carcinoma. *Br J Cancer* 2017;**117**:1631–43.
56. O'Garra A, Vieira P. T(H)1 cells control themselves by producing interleukin-10. *Nat Rev Immunol* 2007;**7**:425–8.
57. Roncarolo MG, Gregori S, Bacchetta R, Battaglia M, Gagliani N. The biology of T regulatory type 1 cells and their therapeutic application in immune-mediated diseases. *Immunity* 2018;**49**:1004–19.
58. Chen W, Jin W, Hardegen N, *et al*. Conversion of peripheral CD4+CD25- naive T cells to CD4+CD25+regulatory T cells by TGF-beta induction of transcription factor Foxp3. *J Exp Med* 2003;**198**:1875–86.
59. Vieira PL, Christensen JR, Minaee S, *et al*. IL-10-secreting regulatory T cells do not express Foxp3 but have comparable regulatory function to naturally occurring CD4+CD25+regulatory T cells. *J Immunol* 2004;**172**:5986–93.
60. Veldman C, Pahl A, Beissert S, *et al*. Inhibition of the transcription factor Foxp3 converts desmoglein 3-specific type 1 regulatory T cells into Th2-like cells. *J Immunol* 2006;**176**:3215–22.